Intelligent Automation & Soft Computing

Tech Science Press

DOI: 10.32604/iasc.2023.031575
Article

A Chaotic Pulse Train Generator Based on Henon Map

Babu H. Soumya[1,*], N. Vijayakumar[2] and K. Gopakumar[3]

[1]College of Engineering, Trivandrum, 695016, India
[2]Government Engineering College, Barton Hill, Trivandrum, 695035, India
[3]APJ Abdul Kalam Technological University, Trivandrum, 695016, India
*Corresponding Author: Babu H. Soumya. Email: soumiyam@gmail.com
Received: 21 April 2022; Accepted: 17 August 2022

Abstract: The Henon map forms one of the most-studied two-dimensional discrete-time dynamical systems that exhibits chaotic behavior. The Henon map takes a point (X_n, Y_n) in the plane and maps it to a new point (X_{n+1}, Y_{n+1}). In this paper, a chaotic pulse generator based on the chaotic Henon map is proposed. It consists of a Henon map function subcircuit to realize the Henon map and another subcircuit to perform the iterative operation. The Henon map subcircuit comprises operational amplifiers, multipliers, delay elements and resistors, whereas, the iterative subcircuit is implemented with a simple design that comprises of an edge forming circuit followed by a monostable multivibrator and a voltage controlled switch without the use of any clock control. The proposed design can be used to realize the Henon map and also to generate a chaotic pulse train, with a controllable time interval and pulse position. The proposed circuit is implemented and simulated using Multisim 13.0 and MATLAB R2019b. The chaotic nature of the generated pulse train and also the time interval between the consecutive pulses is verified by the calculation of its Lyapunov exponents.

Keywords: Chaos; iterated maps; henon map; chaotic pulse train; lyapunov exponents

1 Introduction

Chaotic systems are deterministic nonlinear dynamical systems that consist of a set of possible states, together with a rule that determines the present state in terms of past states. It is required that the rule be deterministic, to uniquely determine the present state from the past states. When the governing rule is applied at discrete times, it is a discrete-time dynamical system or the so-called iterated maps and when the rule is a set of differential equations, it is a continuous-time dynamical system [1]. These systems are characterized by high sensitivity to initial conditions, presence of dense orbits and must be topologically transitive, which makes the system output completely different for even a very small change in the input applied to the system [2]. A chaotic map or the so-called iterated

map is an evolution function exhibiting chaotic behavior, and can be parameterized by a discrete-time or a continuous-time parameter. It mostly takes the form of iterative functions and can be one-dimensional, two-dimensional or multi-dimensional. But much attention is given to one-dimensional and two-dimensional quadratic mappings, as they exhibit all the interesting properties a map can have.

Such pseudo-random behavior of chaotic systems makes these systems highly regarded for various applications like pseudo-random sequence generation, encryption and secure communication. Moreover, these systems are extensively used for the generation of chaotic signals and chaotic pulse train, that can be used as a control signal and modulating signal, and has several applications in cryptography [3], data processing [4], secure communication [5], steganography [6], bio-medical processing and its extended applications [7,8].

Several works have been done in the past for the generation of chaotic pulse train. In 2008, Wang et al. introduced a method to generate chaotic pulse sequence by chaotic phase trajectory [9]. In 1994, Balmforth et al. found that under certain particular conditions, the third-order nonlinear ODE can take the form of a chaotic pulse sequence [10]. Later in 2005, methods were proposed for generating chaotic pulse for reaction-diffusion systems, mainly focused on algorithm implementation and not appropriate for circuit implementation [11]. Dmitriev et al. in 2005 proposed a method to generate the chaotic pulse trains using a dynamical system that uses a periodic signal [12]. In most of these dynamic systems with circuits implemented by resistors, capacitors, monostable multivibrators, analog switches etc. one–dimensional return maps are used. But in these methods, it is difficult or not possible to control the generated pulse parameters like pulse position, pulse interval etc. The major drawback of such a realization is the requirement of an external control signal to drive the circuits and the difficulty in controlling various parameters such as pulse width and frequency of the generated chaotic pulse sequence. In the last decade, another one-dimensional piecewise linear map referred to as the Tent map has been used extensively in these applications [13,14] and such circuit implementations [15,16]. In 2000, Tanaka et al. proposed the voltage mode based integrated circuits of Logistic map and Tent map chaotic generators [17]. In 2009, Campos-Canton et al. proposed a voltage mode based electronic circuit to implement the Tent map [18]. Though these circuits are easy to implement, chaotic pulse sequence could not be produced. Later in 2015, Zhang et al. proposed a chaotic pulse generator based on the Tent map which overcomes the drawbacks of the previous methods and can be used for the generation of chaotic pulse sequence with control over the pulse parameters [19].

However, this article proposes the implementation of a chaotic pulse train based on a two-dimensional chaotic map referred to as the Henon map. In past literatures, only a few one-dimensional chaotic maps like logistic map, Tent map etc. have been realized and analyzed for such applications [18,20,21]. But, very few works have been done to realize the two-dimensional iterated maps, and analyze its chaotic and complex dynamics [22,23]. Even though all the circuits mentioned in these literatures can be used to generate chaotic series, and some of them are even easy to implement, since these methods use periodic clock signals to implement the iterative process, the chaotic pulse train or sequence may not be produced. This article deals with the implementation of a circuit to realize the Henon map and thus generate two sets of chaotic time series and also to generate the chaotic pulse sequence with a control on the pulse parameters like pulse interval and pulse position. Also, the entire circuit is realized more concisely compared to the existing literatures and has a reasonable design without any clock control.

The Henon map forms one of the most studied two-dimensional discrete-time dynamical systems that exhibit chaotic behavior. It was introduced as a simplified model of the Poincare section of Lorenz model [24]. Due to its simple form and interesting chaotic behaviors, the map has always been attractive

as a mathematical model to study deterministic chaos. The map takes a point (X_n, Y_n) in the plane and maps it to a new point (X_{n+1}, Y_{n+1}), where (X_n, Y_n) are the initial conditions or the initial state of the map, whereas, X_{n+1} and Y_{n+1} forms the next state of the map after iteration. The map also depends on two bifurcating parameters 'a' and 'b'. For the classical Henon map, the bifurcating parameters are set to the values, $a = 1.41$ and $b = 0.3$, which keeps the map in the chaotic regime [25]. The Henon map also exhibits a strange horseshoe shaped attractor with a fractal structure, and a constant value for the Jacobian determinant $| J | = - b$. This existence of chaotic behavior and a transversal homoclinic orbit for the map for some specific parameter values was analytically proved by Marotto [26].

2 Circuit Implementation

This article focuses on the circuit implementation of a chaotic pulse generator. A 2-D chaotic Henon map based chaotic pulse train generator is proposed, which does not require an external control signal. The design of the proposed circuit consists of mainly two parts (A) Henon map subcircuit realization (B) a circuit to realize the iterative operation. The Henon map subcircuit realization is done more precisely compared to the ones in the existing literatures whereas, the iterative subcircuit is implemented with a simple design without any clock control. Instead of using an external control signal, an edge signal forming circuit is designed to generate a positive and negative edge signal that, in turn, triggers a monostable multivibrator (MM). Upon triggering, a pulse signal is generated at the output of the MM, which is used to close an analog switch that passes the output of the Henon map to its input.

Fig. 1 shows the overall block diagram of the proposed circuit. It consists of a simple circuit designed to set initial condition for the Henon map, followed by a circuit to realize the Henon map. The Henon map realization is followed by an iterative subcircuit which feeds back the iterated output of the Henon map so that, it serves as the next input to the Henon map.

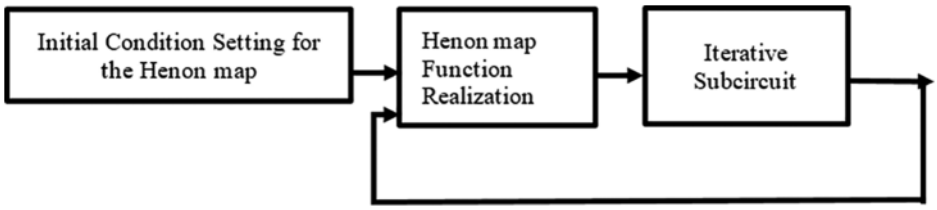

Figure 1: Block diagram of the proposed circuit

2.1 Henon Map Function Subcircuit

The Henon map function takes a point (X_n , Y_n) in the plane and maps it to a new point (X_{n+1}, X_{n+1}) as given by the Eqs. (1) and (2) where (X_n, Y_n) represens the initial conditions of the map and X_{n+1} and Y_{n+1} represent the next state of the map, obtained by iterating the map once. Eqs. (1) and (2) describe a classical Henon map with 'a' and 'b' as the bifurcating parameters. For the chaotic classical Henon map, the value of 'a' is set to 1.41 and 'b' to 0.3, for the Henon map to be in the chaotic regime. The Henon map can be chaotic, intermittent or can even converge to a periodic orbit for other values of 'a' and 'b' [27,28].

$$X_{n+1} = 1 - a\, X_n^2 + Y_n \tag{1}$$

$$Y_{n+1} = b \cdot X_n \tag{2}$$

Fig. 2 shows the circuit diagram of the proposed subcircuit of the Henon map. The Henon map is realized using an operational amplifier U3A, four resistors R_2 to R_5, two multipliers A_1 and A_2, a delay element A_3 and power supplies. Two multipliers A_1 and A_2 are used to set the values of the parameters '*a*' and '*b*'. Since for the classical Henon map, $a = 1.41$ and $b = 0.3$, one of the inputs to the multipliers A_1 and A_2 are set to -1.41 and 0.3 respectively, so as to design the Henon map as described by Eqs. (1) and (2). The operational amplifier U3A, configured in non-inverting mode of operation along with resistors R_2 to R_5, is configured to act as a summing amplifier. In order to make the op-amp output equal to the sum of the inputs at the non-inverting terminal of it, the closed-loop gain of the op-amp is made equal to three, which is equal to the number of summing inputs [29].

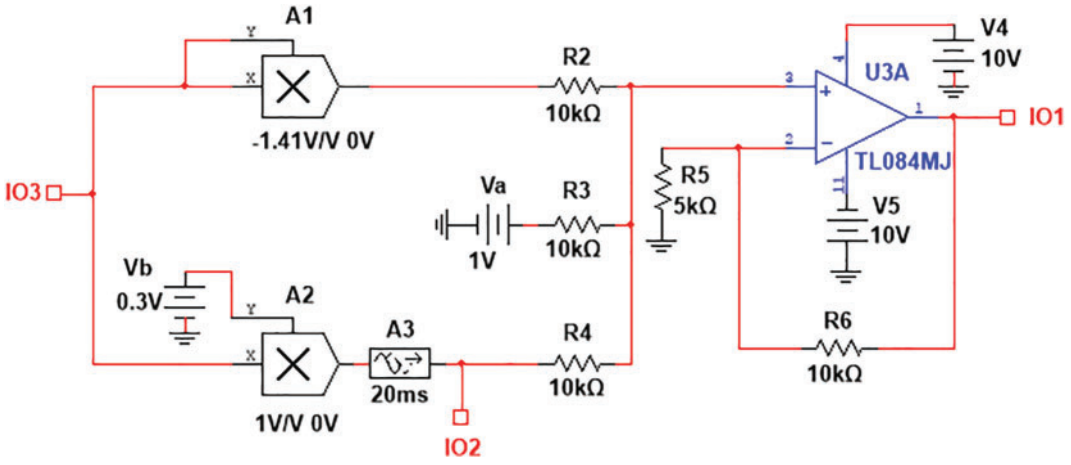

Figure 2: Circuit diagram of the Henon map subcircuit realization

The closed-loop gain of the summing amplifier is given by $A_v = 1 + \left(\frac{R_6}{R_5}\right)$. Since, $A_v = 3$, the values of resistors are chosen to be $R_6 = 10\,\text{K}\Omega$ and $R_5 = 5\,\text{K}\Omega$. Also, if the input resistances R_2, R_3 and R_4 are all made equal, the circulating currents cancel out since they cannot flow into the high impedance non-inverting input of the op-amp and the output voltage of the op-amp becomes equal to the sum of its inputs at the non-inverting terminal. Therefore, $R_2 = R_3 = R_4 = 10\,\text{K}\Omega$. Thus, the map is realized with less number of components when compared to those in the existing literatures. Two sets of chaotic sequences can be generated from the Henon map for a particular value of '*a*' and '*b*', though only one set of sequences (X_0, X_1, X_2, X_3, ...) is utilized in this article to be used as one of the inputs to the edge forming circuit.

2.2 Iterative Function

In this article, an ingenious design consisting of an edge signal forming circuit, a switch and a monostable multivibrator (MM) is used to develop a circuit that performs an iterative operation as described in the Fig. 3. The edge signal generated is used to trigger the MM, that in turn produces the pulse signal at its output. This pulse output from the MM is used as control signal to control the analog switch, that pass on the signal X_{n+1} onto X_n.

3 Working Principle

The overall circuit diagram of the proposed circuit to generate the chaotic pulse train is shown in the Fig. 4. It consists of a simple circuit to set the initial condition of the Henon map followed by the

Henon map realization subcircuit, a comparator circuit using LM311D, a monostable multivibrator CD4538BCM and a voltage-controlled SPST switch S_2.

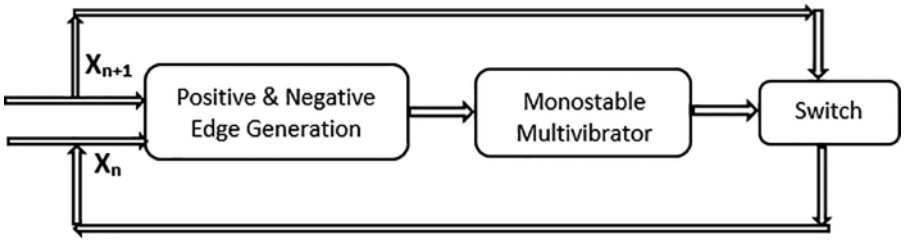

Figure 3: Flow diagram of the proposed iterative operation

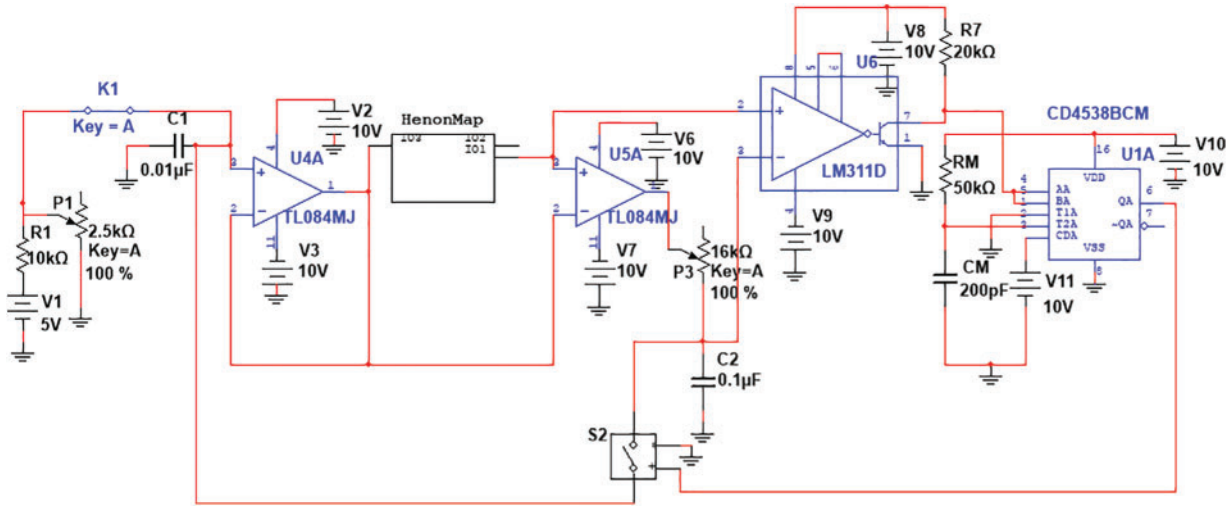

Figure 4: Overall circuit diagram of the proposed circuit

The initial condition X_0 for the Henon map is set using the resistor R_1, Key K_1, capacitor C_1 and the potentiometer P_1. The value of X_0 is selected in the range [0, 1] by suitably selecting the values of the different components, with the switch K_1 closed and then fed as the non-inverting input to an operational amplifier U4A that acts as a voltage follower. The output of the voltage follower is fed as the initial condition of the Henon map. Even though two sets of chaotic sequences are generated from Henon map, only one set of chaotic sequences given by [X_0, X_1, X_2 . . . . .] is taken into consideration to the next stage of the system. Initially, the initial condition X_0, and the iterated output X_1 are fed to the next stage of the system that forms the iterative circuit.

In the implementation of the iterative circuit, the design of the edge forming circuit forms the crucial part. It is implemented by making use of an operational amplifiers U5A, a comparator U6 using LM311D, a switch S_2, a capacitor C_2 and a potentiometer P_3. The initial state X_0, and the corresponding output state of the Henon map, X_{n+1} are fed as inverting and non-inverting inputs of the op amp U5A respectively, whereas the output is connected to a capacitor C_2 through a potentiometer P_3. The voltage across the capacitor C_2 is fed as the inverting input of the comparator circuit using LM311 whereas X_{n+1} forms the non-inverting input of the comparator.

When X_{n+1} is greater than X_n, the op amp U5A outputs a high positive power supply voltage and U6, the comparator circuit produces a high output voltage level. Now, the capacitor C_2 gets charged

through the potentiometer P_3 and when the voltage across the capacitor rises to X_{n+1}, which is in turn fed as the inverting input to the comparator U_6, it produces a low output voltage. This results in the appearance of a falling edge at the output of the comparator. Similarly, when X_{n+1} is lesser than X_n, the op amp U5A produces a low power supply voltage and U6 produces a high voltage level. Now, the capacitor C_2 starts to discharge through the generated negative power supply voltage. When the voltage across the capacitor C_2 discharges to X_{n+1}, the output of the comparator U6 rises to high level, resulting in the appearance of a rising edge at its output. This output of the comparator LM311 is in turn fed as the trigger input to the monostable multivibrator circuit, which results in the generation of the chaotic pulse train. The generated pulse from the MM is used to close the voltage-controlled SPST switch S_2, which in turn passes X_{n+1} to X_n.

Since both positive and negative triggering are used to trigger the monoshot CD4538BCM IC, a dual precision monostable multivibrator is chosen for the circuit, which has two triggering inputs to enable both rising and falling edge triggering. The time period of the output pulse of the MM is controllable with the use of external resistor R_M and capacitor C_M, whose values are designed accordingly. By repeating this process, an iterative process can be thus accomplished.

The time interval between the n^{th} and $(n+1)^{th}$ chaotic pulse generated is denoted by T_n. The expression for evaluating T_n can be obtained by using the basic charging equations of a capacitor 'C' given by Eq. (3), which represents the voltage V_C across a capacitor 'C', with initial voltage V_i, charged from a voltage source V_f through a resistor R [30].

$$V_C = V_f + \left(V_i - V_f\right) e^{-T/RC} \tag{3}$$

In this case, when $X_n < X_{n+1}$, $V_C = X_{n+1}$, $V_i = X_n$ and $V_f = V$ and when $X_n > X_{n+1}$, $V_C = X_{n+1}$, $V_i = X_n$ and $V_f = -V_{DD}$. Thus, based on the charging principle of the capacitor C_2 with initial voltage X_n, getting charged to V_1 through a potentiometer P_3, the time interval T_n can be expressed as

$$\begin{aligned} T_n &= P_3 C_2 \ln\left[\frac{V_1 - X_n}{V_1 - X_{n+1}}\right] \; if \; X_n < X_{n+1} \\ T_n &= P_3 C_2 \ln\left[\frac{V_1 + X_n}{V_1 + X_{n+1}}\right] \; if \; X_n > X_{n+1} \end{aligned} \tag{4}$$

where X_n and X_{n+1} represent the n^{th} and $(n+1)^{th}$ sequence generated from the Henon map and $V_1 = 5$ V, represents the power voltage. From Eq. (4), it is evident that the time interval between the consecutive pulses is directly proportional to the product of P_3 and C_2.

4 Simulation and Analysis

Table 1 summarizes the various components and devices used in the circuit along with its values. First step is the setting of an appropriate value of initial condition for the Henon map in the range [0, 1] by suitably adjusting the values of the potentiometer P_3, resistor R_1 and power supply. In this article, the electronic circuit to generate the chaotic sequences and chaotic pulse train is simulated and analyzed using Multisim 13.0, whereas, the Lyapunov exponents of the generated sequence and the pulse interval between the consecutive pulses are measured using MATLAB R2019b. The simulations were performed for an initial condition of $(X_n, Y_n) = (0.981, 0)$ by setting $P_1 = 2.5\text{K}\Omega$, $R_1 = 10\text{K}\Omega$ and $V_1 = 5$ V. The initial condition specified, was chosen randomly so as to be in the range [0, 1].

Figs. 5a and 5b shows the chaotic waveforms generated from the Henon map, realized with bifurcating parameters $a = 1.41$ and $b = 0.3$, with an initial condition of (0.981, 0). It represents

the generated chaotic output waveforms of X_n and Y_n, indicated in red and green respectively. The figure clearly shows that the generated waveforms vary chaotically, which can be verified further by computing its Lyapunov exponents.

Table 1: Electronic components used in the design of the proposed chaotic pulse generator

Device	Value
R_1, R_2, R_3, R_4, R_6	10KΩ
R_5	5KΩ
R_7	20KΩ
P_1	2.5KΩ
P_3	16KΩ
R_M	50KΩ
C_M	200 pF
C_1	0.01 μF
C_2	0.1 μF
S_2	SPST voltage controlled switch
U1A	CD4538BCM, monostable multivibrator
U3A,U4A,U5A	TL084MJ
U6	LM311D comparator

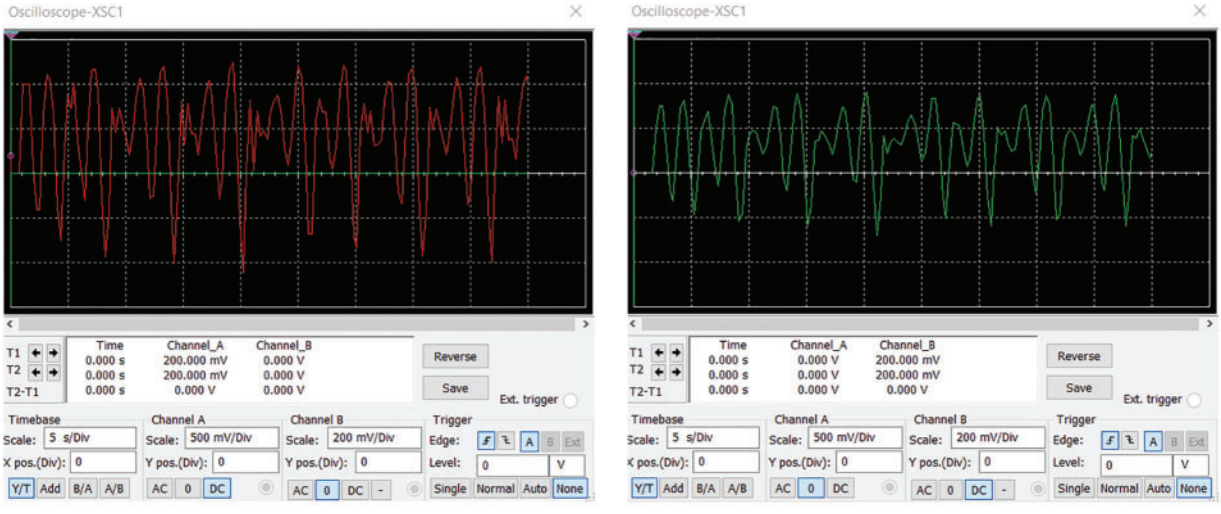

(a) (b)

Figure 5: The chaotic waveforms $\boldsymbol{X}_{n+1}$ and $\boldsymbol{Y}_{n+1}$ generated from the realized Henon map circuit

Fig. 6 shows the Henon attractor obtained from the simulated results X_{n+1} and Y_{n+1} of the Henon map circuit, plotted in Figs. 5a and 5b. It shows the peculiar well-known horseshoe shaped Henon attractor.

The influence of the potentiometer P_3 on the time period of the chaotic series generated is indicated in Fig. 7. It show the waveforms of the Henon map series X_n and the chaotic pulse train P_n, generated

by the test circuit for an initial condition $X_0 = 981$ mV where, the value of the potentiometer is changed from 16 kΩ to 32 KΩ as shown respectively in Figs. 7a and 7b. Based on the previous discussion, as indicated by Eq. (4), the figure clearly indicates that the time period between the generated chaotic pulses is directly proportional to the value of the potentiometer P_3, i.e.; $T_n \alpha P_3$, since the amount of pulse generated with $P_3 = 32\text{k}\Omega$ is twice that is generated with $P_3 = 32\text{k}\Omega$. Also, the values of the generated Henon map series is in good agreement with the theoretical values and that whenever the X_n value mutates, the chaotic pulse appears.

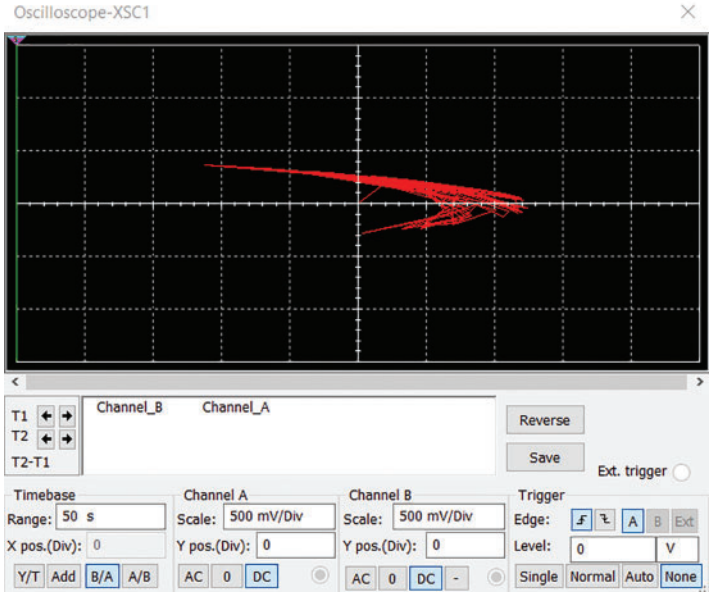

Figure 6: The Henon map attractor obtained from the simulated results of $\boldsymbol{X_{n+1}}$ and $\boldsymbol{Y_{n+1}}$

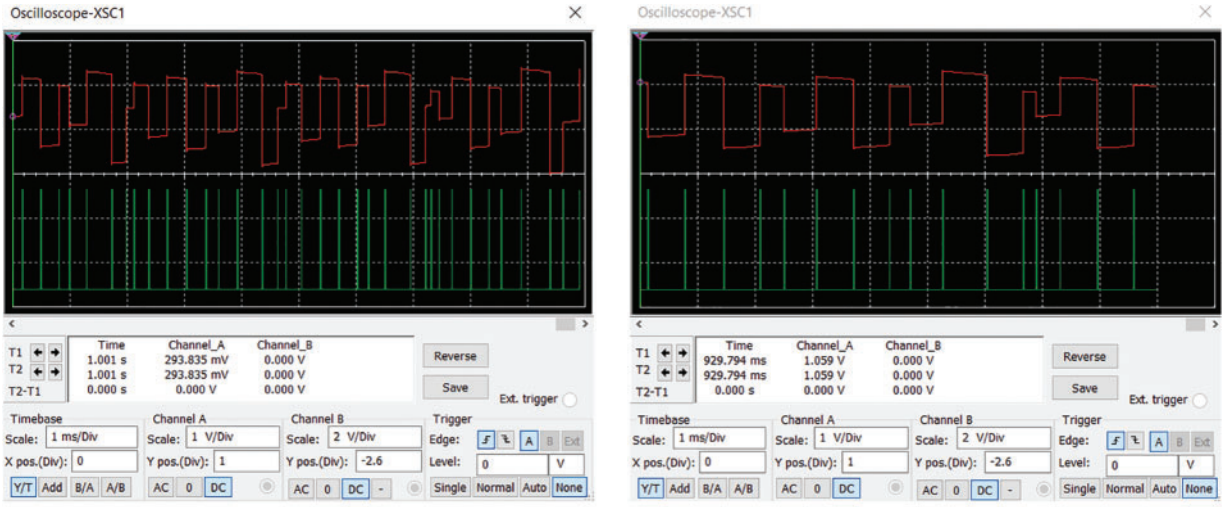

Figure 7: The waveforms of Henon map series X_n (red) and chaotic pulse train $\boldsymbol{P_n}$ (green) generated from the circuit for initial condition $\boldsymbol{X_0} = 981$ mV with (a) $P_3 = 16\,\text{K}\Omega$ (b) $P_3 = 32\,\text{K}\Omega$

The chaotic nature of the pulse train generated from the MM can be verified by calculating its Lyapunov exponents [31]. The Lyapunov exponents provide a quantitative as well as qualitative characterization of dynamical systems and are also related to the nearby orbit's quick divergence or convergence in phase space. The Lyapunov exponents of a discrete-time dynamical system $X_{n+1} = f(X_n)$ is expressed as $L(X_0) = \lim_{n\to\infty} \frac{1}{n} \sum_{i=0}^{n-1} \ln |f'(X_i)|$. If $L > 0$, then $\{X_n\}$ denotes a chaotic sequence. The Lyapunov exponents of both, the pulse train generated from the MM and the time interval between n^{th} and $n+1^{th}$ pulse, represented by T_n can be calculated using the method proposed by Wolf et al. [32]. Figs. 8a and 8b show the plot of Lyapunov exponents of the pulse train generated and T_n against the bifurcating parameter 'a' calculated from the time series generated from the realized Henon map for an initial condition of $(X_0, Y_0) = (0.982, 0.294)$ respectively. The figure clearly indicates that the Lyapunov exponents of both X_n and T_n are positive, thus indicating the chaotic nature of the generated pulse train [33].

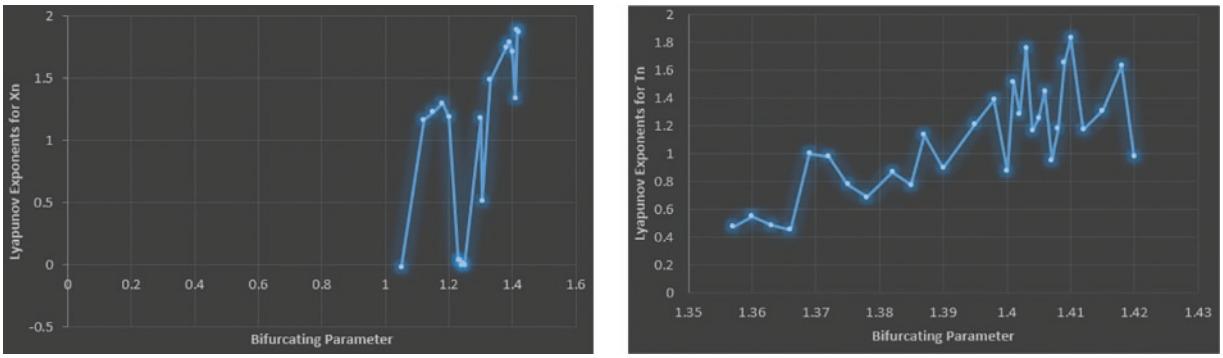

Figure 8: (a, b) Plot of Lyapunov Exponents calculated for $\boldsymbol{X_n}$ and $\boldsymbol{T_n}$ with the bifurcating parameter from the time series for an initial condition $\boldsymbol{X_0} = 0.982$ V and $\boldsymbol{Y_0} = 0.294$ V

5 Comparison with Other Benchmark Algorithms

In the electronic circuit designed, simulated and analyzed in the article, less number of components are utilized to implement the overall circuit thus, when compared to other benchmark circuits, the overall circuit is more concisely realized. The same circuit can be used to realize the Henon map and also to generate two sets of chaotic series and a chaotic pulse train. Moreover, the position and time interval of the generated chaotic pulse are controllable by varying the variable components used in the design. Another important feature of the design is the implementation of a circuit to perform iterative operation. To implement an iterative operation, a reasonable design comprising an edge forming circuit, analog switch and monostable multivibrator is employed which eliminates the need of a periodic clock control in contrast to existing works.

6 Conclusion

In this article, a two-dimensional Henon map based chaotic sequence and pulse generator is proposed. The designed and simulated circuit can be used to realize the Henon map function and also to generate two sets of chaotic sequences and a chaotic pulse train. The proposed circuit is simple since less number of components are used to implement the system. The circuit is designed using various electronic components such as operational amplifier, comparator, monostable multivibrator,

analog switch and other passive components. The key feature of this realization is that the generated chaotic pulse train from the monoshot multivibrator can be controlled in terms of pulse interval and also pulse position, by changing the values of various electronic components used in the circuit. The chaotic nature of both, the generated pulse train and the time interval between the consecutive pulses, is verified by its calculated positive Lyapunov exponents and plotted against the bifurcating parameter.

Funding Statement: The authors received no specific funding for this study.

Availability of Data and Materials: The data used to support the findings of the study are available from the corresponding author upon request.

Conflicts of Interest: The authors declare that they have no conflicts of interest to report regarding the present study.

References

[1] K. T. Alligood, T. D. Sauer and J. A. Yorke, "One-dimensional maps," in *CHAOS An Introduction to Dynamical Systems*, 1st ed., vol. 1. New York: Springer-Verlag, pp. 1–3, 1997.

[2] J. Banks, J. Brooks, G. Cairns, G. Davis and P. Stacey, "On devaney's definition of chaos," *The American Mathematical Monthly*, vol. 99, no. 4, pp. 332–334, 1992.

[3] H. J. Gao, Y. S. Zhang, S. Y. Liang and D. Q. Li, "A new image encryption algorithm based on hyper-chaos," *Solitons and Fractals*, vol. 29, no. 12, pp. 393–399, 2006.

[4] H. Torikai, T. Saito and W. Schwarz, "A chaotic pulse generator and sawtooth control for information processing," in *Proc. IEEE Int. Symp. on Circuits and Systems (ISCAS)*, Hong Kong, China, pp. 729–735, 1997.

[5] Z. J. Yao, Q. H. Meng, G. W. Li and P. Lin, "Non-crosstalk real-time ultrasonic range system with optimized chaotic pulse position-width modulation excitation," in *Proc. IEEE Ultrasonics Symp. (IUS)*, Beijing, China, pp. 729–732, 2008.

[6] X. Liao, Y. Yu, B. Li, Z. Li and Z. Qin, "A new payload partition strategy in color image steganography," *IEEE Transactions on Circuits and Systems for Video Technology*, vol. 30, no. 3, pp. 685–696, 2020.

[7] T. -L. Liao, H. -C. Chen, C. -Y. Peng and Y. -Y. Hou, "Chaos-based secure communications in biomedical information application," *Electronics*, vol. 10, pp. 359–379, 2021.

[8] A. Hobiny, F. Alzahrani, I. Abbas and M. Marin, "The effect of fractional time derivative of bioheat model in skin tissue induced to laser irradiation," *Symmetry*, vol. 12, no. 4, Article No. 602, pp. 1–10, 2020.

[9] Y. W. Wang, L. P. Wang, S. Yu, L. Zhang, D. M. Yan *et al.,* "Chaotic pulses for diffusion systems," in *Proc. Int. Conf. on Signal Processing (ICSP)*, Beijing, no. 7, pp. 1892–1896, 2008.

[10] N. J. Balmforth, G. R. Ierley and E. A. Spiegel, "Chaotic pulse trains," *SIAM Journal on Applied Mathematics*, vol. 54, no. 5, pp. 129–134, 1994.

[11] Y. Nishiura, D. Ueyama and T. Yanagita, "Chaotic pulses for discrete reaction diffusion systems," *SIAM Journal on Applied Dynamical Systems*, vol. 4, no. 3, pp. 733–754, 2005.

[12] A. S. Dmitriev, E. V. Efremova and L. V. Kuz'min, "Chaotic pulse trains generated by a dynamical system driven by a periodic signal," *Technical Physics Letters*, vol. 11, no. 33, pp. 961–963, 2005.

[13] T. Addabbo, M. Alioto, A. Fort, S. Rocchi and V. Vignoli, "The digital tent map: Performance analysis and optimized design as a low-complexity source of pseudorandom bits," *IEEE Transactions on Instrumentation and Measurement*, vol. 55, no. 5, pp. 1451–1458, 2006.

[14] Y. Wang, K. W. Wong, X. F. Liao and T. Xiang, "A block cipher with dynamic S-boxes based on Tent map," *Communications in Nonlinear Science and Numerical Simulation*, vol. 14, no. 7, pp. 3089–3093, 2009.

[15] J. T. Bean and P. J. Langlois, "A current mode analog circuits for Tent maps using piecewise linear functions," in *Proc. IEEE Int. Symp. on Circuits and Systems (ISCAS)*, London, UK, vol. 6, pp. 125–129, 1994.

[16] P. Dudek and V. D. Juncu, "Compact discrete-time chaos generator circuit," *Electronics Letters*, vol. 39, no. 20, pp. 1431–1432, 2003.
[17] H. Tanaka, S. Sato and K. Nakajima, "Integrated circuits of map chaos generators," *Analog Integrated Circuits and Signal Processing*, vol. 25, no. 3, pp. 329–335, 2000.
[18] I. Campos-Canton, E. Campos-Canton, J. S. Murguia and C. Rosu, "A simple circuit realization of the Tent map," *Chaos, Solitons & Fractals*, vol. 42, no. 1, pp. 12–16, 2009.
[19] T. -F. Zhang, S. -L. Li, R. -J. Ge, M. Yuan, G. Gui *et al.,* "A chaotic pulse sequence generator based on the Tent map," *IEICE Electronics Express*, vol. 12, no. 16, pp. 1–10, 2015.
[20] E. D. M. Hernandez, G. Lee and N. H. Farhat, "Analog realization of arbitrary one-dimensional maps," *IEEE Transactions on Circuits System I:Fundamental Theory Applications*, vol. 50, no. 12, pp. 1538–1547, 2003.
[21] M. Suneel, "Electronic circuit realization of the Logistic map," *Sadhana*, vol. 31, no. 1, pp. 1–14, 2006.
[22] M. Garcia-Martinez, I. Campos-Canton, E. Campos-Canton and S. Celikovsky, "Difference map and its electronic circuit realization," *Nonlinear Dynamics*, vol. 73, pp. 819–830, 2013.
[23] O. O. Aybar, I. K. Aybar and A. S. Hacinliyan, "Stability and bifurcation in the Henon map and its generalizations," *Chaotic Modeling and Simulation (CMSIM)*, vol. 4, pp. 529–538, 2013.
[24] J. F. Heagy, "A physical interpretation of the H´enon map," *Physica. D*, vol. 57, no. 3, pp. 436–446, 1992.
[25] M. Henon, "A two–dimensional mapping with a strange attractor," *Communications in Mathematical Physics*, vol. 50, no. 1, pp. 69–77, 1976.
[26] F. R. Marotto, "Chaotic behaviour in the Henon mapping," *Communications in Mathematical Physics*, vol. 68, no. 2, pp. 187–194, 1979.
[27] W. F. H. Al-Shameri, "Dynamical properties of the H´enon mapping," *International Journal of Mathematical Analysis*, vol. 6, no. 49, pp. 2419–2430, 2012.
[28] M. Cai, "Complex dynamics in generalized Henon map," *Discrete Dynamics in Nature and Society*, vol. 2015, Article ID 270604, pp. 1–18, 2015.
[29] D. Chattopadhyay and P. C. Rakshit, *Electronics Fundamentals and Applications*, 12th ed., New Delhi: New Age International (P) Limited Publishers, pp. 336–339, 2014.
[30] K. Gopakumar, "Capacitor," in *Design and Analysis of Electronic Circuits*, 2nd ed., Kollam: Phasor Books, pp. 2–4, 2004.
[31] M. Sano and Y. Sawada, "Measurements of the Lyapunov spectrum from chaotic time series," *Physical Review Letters*, vol. 55, no. 10, pp. 1082–1085, 1985.
[32] A. Wolf, J. B. Swift, H. L. Swinney and J. A. Vastano, "Determining Lyapunov exponents from a time series," *Physica D:Nonlinear Phenomena*, vol. 16, no. 3, pp. 285–317, 1985.
[33] A. Dabrowski, T. Sagan, V. Denysenko, M. Balcerzak, S. Zarychta *et al.,* "Alternative methods of the largest lyapunov exponent estimation with applications to the stability analyses based on the dynamical maps—Introduction to the method," *Materials*, vol. 14, no. 23, pp. 7197–7212, 2021.